# Low damping in epitaxial sputtered iron films

C. Scheck,[a] L. Cheng, and W. E. Bailey
*Materials Science and Engineering Program, Department of Applied Physics and Applied Mathematics, Columbia University, 500 W 120th Street, New York, New York 10027*

(Received 16 February 2006; accepted 22 May 2006; published online 22 June 2006)

We show that sputtered, pure epitaxial iron films can have high-frequency loss as low as, or lower than, any known metallic ferromagnetic heterostructure. Minimum 34 GHz ferromagnetic resonance linewidths of 41±2 Oe are demonstrated, some ~5%–10% lower than the previous minimum reported for molecular beam epitaxially deposited Fe. Intrinsic and extrinsic damping have been separated over 0–40 GHz, giving a lower bound for intrinsic LL(G) relaxation rates of λ or $G=85\pm5$ MHz ($\alpha=0.0027\pm0.0001$) and for extrinsic $\eta\sim30-50$ MHz. Swept-frequency measurements indicate the potential for integrated frequency domain devices with $Q>100$ at 30–40Ghz. © *2006 American Institute of Physics*. [DOI: 10.1063/1.2216031]

Attaining low damping $\alpha$ or relaxation rate λ is an essential materials goal for high-frequency applications of magnetic heterostructures. Nanoscale spin electronic sensors operating above 1 GHz have signal-to-noise ratios (SNR) which depend inversely on the damping constant $\alpha$ and are independent of spin transport parameters.[1] Integrated magnetic frequency domain devices have frequency linewidths ($\Delta\omega/2\pi$) limited fundamentally by the Landau-Lifshitz-(Gilbert) relaxation rate $\lambda(=G)=\alpha\gamma M_s$,[2] where $\gamma$ is the gyromagnetic ratio. It is timely to determine how low relaxation rates can be made in a ferromagnetic thin film, particularly using widely accessible deposition techniques such as sputtering.

Relaxation processes expressed phenomenologically in $\alpha$ (Ref. 3) can be divided into extrinsic and intrinsic types: extrinsic damping results from microstructure; intrinsic damping results from spin-orbit coupling. The two effects can be separated through variable-frequency ferromagnetic resonance (FMR) measurements, through $\Delta H_{pp}=\Delta H_0+(2/\sqrt{3})\alpha/\gamma$.[5] $\alpha$ in this context expresses intrinsic processes, and Δ expresses inhomogeneous broadening due, e.g., to line defects.[6]

The lowest overall linewidths have been seen in the ultrathin molecular beam epitaxially (MBE) deposited Fe films of Prinz *et al.*, with a 35 GHz $\Delta H_{pp}=45$ Oe (1.29 Oe/GHz) seen in ultrathin Fe(100) deposited on ZnSe(100) epilayers.[7] Intrinsic and extrinsic losses were not separated in the prior work, carried out at a single frequency. Fe also possesses the lowest known *intrinsic* damping constant of any metallic ferromagnet, with a range of λ quoted as $\lambda=70-140$ MHz ($\alpha=0.002-0.004$) in FMR measurement to 40 GHz.[8] The distribution in observed λ ($G$) has been attributed to the presence of point defects which create additional noise in the spin orbit interaction.[9] Variable frequency FMR estimates of $\alpha$ over this range, through $\partial\Delta H/\partial\Delta\omega$, have typically uncovered values of $100\ \text{MHz}\leqslant\lambda\leqslant140$ MHz in high-quality MBE (Refs. 6 and 10) or sputtered films.[11]

In this work, we report UHV sputtered epitaxial pure Fe(100)(15 nm)/Ti(2 nm) films on MgO(100) which show FMR linewidths of $\Delta H_{pp}=41\pm2$ Oe at 34 GHz (1.20 Oe/GHz), some 5%–10% lower than the narrowest linewidths seen to date in MBE deposited films. Variable frequencies of 0–40 GHz FMR identify $\lambda=85\pm5$ MHz ($\alpha=0.0027\pm0.0001$) and $\Delta H_0\sim6\pm2$ Oe for these thin films; a role of eddy current damping is identified in $\alpha$ of thicker Fe films. Swept-frequency measurements demonstrate the potential for field-tunable ~35 GHz filters with $Q>100$, an order of magnitude better than that achieved previously in Fe.

Fe (8–75 nm) thin films were deposited on polished MgO(001) substrates using dc magnetron UHV sputtering at a base pressure of $3.0\times10^{-9}$ Torr. Pressures immediately prior to deposition after sample introduction were typically $1.0\times10^{-8}$ Torr. Substrates were held at 200 °C during sputter deposition at $4\times10^{-3}$ Torr using *in situ* getter-purified Ar, 300 W power for 2 in. targets, and 10 cm target-substrate spacing. Growth rates of ~6 Å/s were measured by a quartz crystal microbalance and *ex situ* profilometry. Films were capped with 2 nm sputtered Ti to protect the surface from oxidation. Rocking curve half-widths measured for 50 nm films were very low, only 0.5°, and roughly independent of deposition temperature over the range of 200–300 °C. Results for ion beam sputtered $Ni_{81}Fe_{19}$ (48 nm) are plotted for comparison; see Ref. 12 for deposition conditions.

Broadband FMR measurements were carried out using microwave frequencies in the range of 4–40 GHz generated by a synthesized sweep generator operating in cw mode. Microwaves were applied to the samples through a coplanar waveguide (CPW) for the range of 4–18 GHz (Ref. 3) and a shorted *K*-band rectangular waveguide for higher frequencies, with a diode detector in transmission and reflection, respectively. Derivative spectra $\Delta\chi''/\Delta H$ were recorded using ac field modulation (<±2 G) and lock-in detection.[13] Swept-field and swept-frequency measurements were both carried out at room temperature.

A representative FMR spectrum for thin (8 or 15 nm) Fe films at 34 GHz is shown in Fig. 1. The film is measured with $H$ applied along the ⟨110⟩ hard axis, along MgO⟨100⟩. The derivative spectrum is shown to be symmetric, with Lorenzian fit indicated and peak-to-peak linewidth measured at $\Delta H_{pp}=41\pm2$ Oe.

Peak-to-peak FMR linewidths $\Delta H_{pp}$ versus frequency $\omega/2\pi$ were plotted for all samples (Fig. 2) to determine the Landau-Lifshitz-Gilbert (LLG) damping constant $\alpha$ and the

[a]Electronic mail: cs2311@columbia.edu

 © 2006 American Institute of Physics
Downloaded 14 Jul 2011 to 128.59.62.83. Redistribution subject to AIP license or copyright; see http://apl.aip.org/about/rights_and_permissions

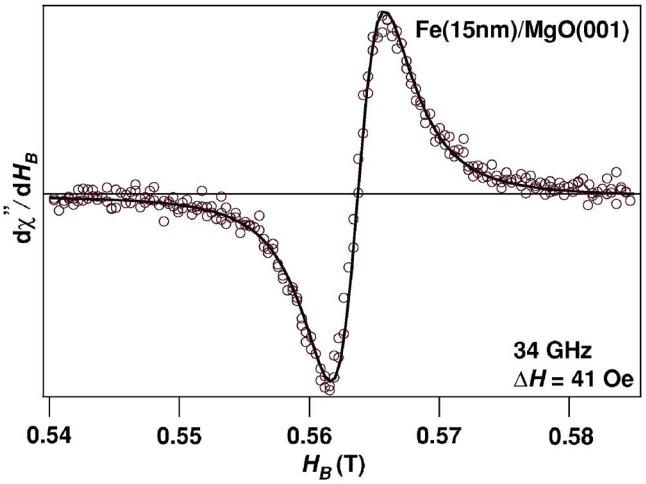


FIG. 1. (Color online) 34 GHz FMR spectrum, with Lorenzian fit, for epitaxially sputtered MgO(001)/Fe(15 nm)/Ti(2 nm). See text for details.

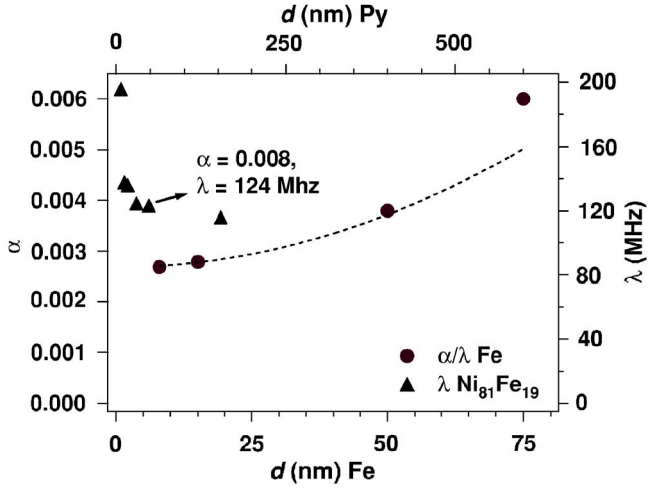


FIG. 3. Extracted damping constant $\alpha$ (left) and relaxation rate λ for epitaxial Fe films. The dashed line shows a calculated contribution of eddy currents to λ [Eq. (1)]. λ for $Ni_{81}Fe_{19}$ is plotted for comparison. See text for details.

inhomogeneous broadening $\Delta H_0$. From the slope $\partial \Delta H / \partial \Delta \omega$, we find a minimum $\alpha = 0.0027 \pm 0.0001$ for thin Fe ($<15$ nm). $\alpha = 0.0075$ is measured for $Ni_{81}Fe_{19}$ (48 nm), consistent with the lower bound of typical values and characteristic of high quality films. Relaxation rates λ are converted from $\alpha$ measurements using $g_{\text{eff}} = 2.09$ (Ref. 8), $4\pi M_s^{Ni_{81}Fe_{19}} = 10.6$ kG, and $4\pi M_s^{Fe} = 21.6$ kG, and plotted for comparison. λ reaches a minimum of $85 \pm 5$ MHz for epitaxial Fe and $120 \pm 10$ MHz for $Ni_{81}Fe_{19}$. Inhomogeneous broadening is negligible for $Ni_{81}Fe_{19}$, with $\Delta H_0 = 2 \pm 2$ Oe, and reaches a minimum of $\Delta H_0 = 6 \pm 2$ Oe for 15 nm Fe.

An increasing trend in $\alpha$ with thickness can be seen for Fe films thicker than 15 nm. We have compared the increase in λ with a standard theory of eddy current damping,[14] which predicts a quadratic increase in Gilbert-type (proportional to $\omega$) linewidth with film thickness $t$:

$$\lambda_{\text{eddy}} = \frac{\sigma}{12}(4\pi\gamma M_s)^2 \left(\frac{t}{c}\right)^2, \tag{1}$$

where $\sigma$ is the conductivity (Hz for cgs units) and $c$ the speed of light in vacuum. $\sigma$ values used for Fe and $Ni_{81}Fe_{19}$ were, respectively, $9.11 \times 10^{16}$ Hz ($\rho = 10$ $\mu\Omega$ cm from four-point-probe measurement) and $4.5 \times 10^{16}$ Hz ($\rho = 20$ $\mu\Omega$ cm). An order of magnitude agreement is found with the increase in λ for Fe films to 75 nm (Fig. 3); the $Ni_{81}Fe_{19}$ data are plotted with a thickness scale compressed by the ratio of the prefactors for the two materials (~8), indicating an expected delayed onset of eddy current damping (>200 nm) for $Ni_{81}Fe_{19}$. A thickness-dependent increase of the inhomogeneous term $\Delta H_0$ from 6 to 30 Oe with increasing Fe thickness may originate in a higher concentration of strain-relaxing dislocations for thicker films.[6]

The advantage of swept-$\omega$ FMR measurement for extracting total relaxation rates $\eta$ has been pointed out by Patton.[2] At low frequency ($H \ll 4\pi M_s$), the relaxation/scattering rate $\eta$ can be measured independent of geometry as

$$\Delta\omega_{\text{pp}} \cong (2/\sqrt{3})\eta, \tag{2}$$

where $\eta = 1/\tau$, giving the decay time as $\exp -\eta t$ in a time-domain experiment,[3] and where $\eta_G = 2\pi\lambda$ in the absence of extrinsic relaxation ($\Delta H_0 = 0$). More generally, in the presence of inhomogeneous broadening and at higher frequency, the frequency linewidth is given by[15]

$$\Delta\omega_{\text{pp}} = (\alpha\gamma/\sqrt{3} + \gamma^2 \Delta H_0 / 4\pi f)(2H + 4\pi M_s - K_1/M_s), \tag{3}$$

with $K_1$ the anisotropy constant, assuming cubic anisotropy only ($K_u = 0$). Figure 4 shows a plot of the peak-to-peak swept-$f$ FMR linewidths versus frequency for Fe (8 and 50 nm) and $Ni_{81}Fe_{19}$ (48 nm) films. The prediction from Eq. (3), using experimental $\alpha$ and $\Delta H_0$ from swept-field measurements, are plotted with the data. It can be seen that the swept-frequency measurements agree, through model (3), quite well with the swept-field measurements. Application of this model to the 15 nm Fe film indicates a low extrinsic scattering rate $\eta_{\text{extrinsic}}$ (where $\eta_{\text{total}} = \eta_G + \eta_{\text{extrinsic}}$) of ~30 MHz at 30–40 GHz.

In principle, CPW measurements of FMR may contain inhomogeneous linewidths resulting from the nonuniformity of the rf field. According to the analysis of Mosendz *et al.*, these linewidth contributions would be 6 Oe for 15 nm Fe and 9 Oe for 50 nm $Ni_{81}Fe_{19}$ in our measurements. However,

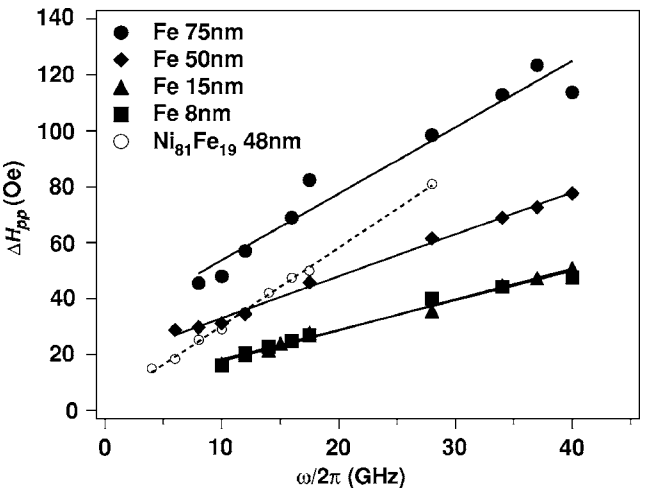


FIG. 2. Frequency dependent peak-to-peak FMR linewidths $\Delta H_{\text{pp}}$ for epitaxially sputtered MgO(100)/Fe(t), 8 nm $< t <$ 75 nm, with linear fits to extract $\alpha$. Data from polycrystalline $SiO_2/Ni_{81}Fe_{19}$(48 nm) are plotted for comparison.

Downloaded 14 Jul 2011 to 128.59.62.83. Redistribution subject to AIP license or copyright; see http://apl.aip.org/about/rights_and_permissions

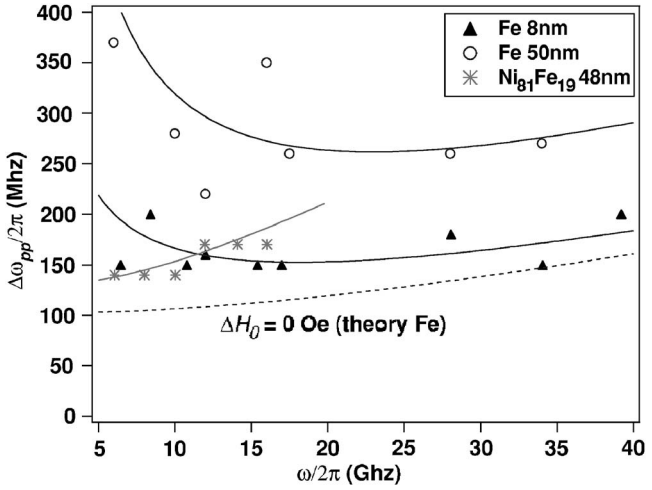


FIG. 4. Swept-frequency FMR linewidths $\Delta\omega_{pp}/2\pi$ for 8 and 50 nm epitaxial Fe; 48 nm (asterisk) $Ni_{81}Fe_{19}$ is shown for comparison. The prediction from Eq. (3), using experimental $\alpha$ and $\Delta H_0$ from swept-field measurements, are plotted with the data.

the latter value is far too large to be contained in the error of our measurements of zero inhomogeneous linewidth for $Ni_{81}Fe_{19}$ (Fig. 2), and the former would account for the whole of the inhomogeneous linewidth for thin Fe. It is possible that our use of photoresist passivation spacing ($\sim 10$ $\mu$m thickness) smooths out the rf field inhomogeneities. Otherwise, the absence of this contribution is not explained. We note, however, the similarity of estimated $\Delta H$ from $K$-band (shorted) waveguide measurements in Fig. 2, which should be immune from this effect.

The observed low extrinsic relaxation rates are a plausible result of the excellent crystalline quality in the ultrathin epitaxial sputtered Fe films. Inhomogeneous broadening is more typically measured on the order of $\Delta H_0 = 50$ Oe,[16] compared with the best of $\Delta H_0 = 6$ Oe seen here. X-ray diffraction rocking curves of the (200) peak on our films show full width at half maxima (FWHM) as low as 0.6°; more standard values for seeded epitaxy in sputtering for this system are 1.1°.[17] Moreover, easy-axis along ($\langle 100 \rangle$) coercivities $H_c$ measured by vibrating-sample magnetometry are 2.1 Oe compared with 3.7 Oe in Ref. 7 in thinner films (50 nm here vs 320 nm for MBE). The inhomogeneous linewidth is the lowest we are aware of in sputtered Fe films. Lower values (to $\Delta H_0 = 0$) have been seen in MBE deposited films, but accompanied by a significantly higher $\lambda$ ($G$) of 124 MHz,[18] translating to a $\sim 30\%$ higher 35 GHz linewidth.

Finally we comment on applications. Favorable epitaxial structures in sputtered Fe/MgO/Fe junctions have resulted in very high tunneling magnetoresistance;[19] our results indicate that low $\alpha$ and high $\Delta R/R$ may coexist. Additionally, the low 35 GHz frequency linewidths seen in our epitaxial Fe films could translate directly to high half-power $Q$ in a frequency domain device. One example is a tunable band stop filter based on FMR. We see $\omega/\Delta\omega_{1/2} = 140$ in our films, roughly an order of magnitude higher than that realized to date in Fe device structures.[20]

The authors thank Z. Frait for helpful discussions. This work was supported by the Army Research Office under Contract Nos. DA-ARO-W911NF0410168, DAAD19-02-1-0375, and 43986-MS-YIP, and has used the shared experimental facilities that are supported primarily by the MRSEC program of the National Science Foundation under NSF-DMR-0213574.

[1] N. Smith and P. Arnett, Appl. Phys. Lett. **78**, 1448 (2001).
[2] C. Patton, J. Appl. Phys. **39**, 3060 (1968).
[3] T. Silva, C. Lee, T. Crawford, and C. Rogers, J. Appl. Phys. **85**, 7849 (1999).
[4] V. Kamberský, Can. J. Phys. **48**, 2906 (1970).
[5] B. Heinrich, in *Ultrathin Magnetic Structures: Fundamentals of Nanomagnetism*, edited by B. Heinrich and J. A. C. Bland (Springer, Berlin, 2005), Vol. III, Chap. 5, pp. 143–210.
[6] G. Woltersdorf and B. Heinrich, Phys. Rev. B **69**, 184417 (2004).
[7] G. Prinz, B. Jonker, J. Krebs, J. Ferrari, and F. Kovanic, Appl. Phys. Lett. **48**, 1756 (1986).
[8] M. Stearns, *Landolt-Borstein Tables* (Springer, Dusseldorf, 1990), Chap. III-13: 1.1.2.10, pp. 86–91.
[9] V. L. Safonov and H. N. Bertram, J. Appl. Phys. **58**, 5611 (2003).
[10] W. Platow, A. Ansimov, G. Dunifer, M. Farle, and K. Baberschke, Phys. Rev. B **58**, 5611 (1998).
[11] P. Lubitz, S. F. Cheng, and F. Rachford, J. Appl. Phys. **93**, 8283 (2003).
[12] S. Reidy, L. Cheng, and W. Bailey, Appl. Phys. Lett. **82**, 1254 (2003).
[13] B. Heinrich and J. Cochran, Adv. Phys. **42**, 523 (1993).
[14] J. Lock, Br. J. Appl. Phys. **17**, 1645 (1966).
[15] O. Mosendz, B. Kardasz, D. S. Schmool, and B. Heinrich, J. Magn. Magn. Mater. **300**, 174 (2006).
[16] F. Schreiber, J. Pflaum, Z. Frait, T. Mughe, and J. Pelzl, Solid State Commun. **93**, 965 (1995).
[17] G. Harp and S. Parkin, Thin Solid Films **288**, 315 (1996).
[18] R. Urban, G. Woltersdorf, and B. Heinrich, Phys. Rev. Lett. **87**, 217204 (2001).
[19] S. Yuasa, T. Nagahama, A. Fukushima, Y. Suzuki, and K. Ando, Nat. Mater. **3**, 868 (2004).
[20] B. Kuanr, Z. Celinski, and R. Camley, Appl. Phys. Lett. **83**, 3969 (2003).

Downloaded 14 Jul 2011 to 128.59.62.83. Redistribution subject to AIP license or copyright; see http://apl.aip.org/about/rights_and_permissions